



UNICA

UNIVERSITÀ  
DEGLI STUDI  
DI CAGLIARI



Università di Cagliari

UNICA IRIS Institutional Research Information System

**This is the Author's *accepted* manuscript version of the following contribution:**

Luca Poluzzi, Luca Tavasci, Enrica Vecchi and Stefano Gandolfi, Impact of Multiconstellation on Relative Static GNSS Positioning, Journal of Surveying Engineering, vol. 142, n. 2, 2021. © 2021 American Society of Civil Engineers

This material may be downloaded for personal use only. Any other use requires prior permission of the American Society of Civil Engineers. This material may be found at

<https://ascelibrary.org/doi/10.1061/%28ASCE%29SU.1943-5428.0000351>

**The publisher's version is available at:**

[https://dx.doi.org/10.1061/\(ASCE\)SU.1943-5428.0000351](https://dx.doi.org/10.1061/(ASCE)SU.1943-5428.0000351)

**When citing, please refer to the published version.**

# Impact of Multiconstellation on Relative Static GNSS Positioning

Luca Poluzzi, Ph.D.<sup>1</sup>; Luca Tavasci, Ph.D.<sup>2</sup>; Enrica Vecchi<sup>3</sup>; and Stefano Gandolfi, Ph.D.<sup>4</sup>

**Abstract:** Until a few years ago, a precise survey was only possible using GPS and GLONASS constellations, but the result was not guaranteed under conditions of poor sky visibility, as in urban canyons. Currently, the number of Global Navigation Satellite System (GNSS) satellites in orbit has strongly increased thanks to the great evolution of the Galileo and the Beidou constellations. In this paper, we investigate the impact of using different constellations and their combinations, in static positioning with the classical differencing approach. For this purpose, two distinct baselines of different lengths (10 and 60 km) were processed using commercial software over a period of one year (2018.24–2019.24). Data were acquired by permanent stations belonging to the European Permanent Network (EPN) network providing 24-h observing sessions. Two datasets were tested, one consisting of 24-h Receiver Independent Exchange Format (RINEX) files and the other considering only 2-h sessions of data acquisition. In both cases, a one-year-long time span has been considered. The baselines were processed considering each of the four GNSS constellations and a series of combinations, for a total of eight solutions. Results have been evaluated looking at the accuracy and repeatability of the coordinates, together with the main constellation parameters. During the analyzed period the number of contemporary visible satellites of the BeiDou constellation was still too poor over the considered area, and therefore this constellation did not provide comparable precisions in respect to the others. Positioning precision provided by the Galileo constellation has shown to be very close to those given by GPS or GLONASS, with a significant difference only on the height component, especially in the case of processing 2-h data. As for 24-h observing sessions, the use of multiconstellation observables actually leads to small improvements in precision with respect to the use of GPS data only, mainly appreciable considering the vertical component. The GPS-Galileo combination gives quite the same performances of the global positioning system-Global Navigation Satellite System (GPS-GLONASS) one, but it can potentially take advantage of the integrity message provided by the European constellation. DOI: [10.1061/\(ASCE\)SU.1943-5428.0000351](https://doi.org/10.1061/(ASCE)SU.1943-5428.0000351). © 2021 American Society of Civil Engineers.

## 23 Introduction

Satellite positioning has become a widely used tool for many civilian and scientific applications thanks to its flexibility in terms of both accuracy and costs. In the era of multiconstellation Global Navigation Satellite Systems (GNSSs), several studies have been done to assess the performances of each constellation and their different combinations. In addition to the NAVSTAR-GPS constellation, the Russian GLObal NAVigation Satellite System (GLONASS), the European Galileo, and the Chinese BeiDou are operational. Other satellite positioning systems like the Japanese Quasi-Zenith satellite system (QZSS) or the Indian regional

navigation satellite system (IRNSS) are operating only in their regional areas. Despite these global satellite systems being designed to provide similar accuracies in good operational conditions, the possibility for combining observables from all the constellations should overcome some of the weaknesses of GNSS positioning under suboptimal conditions.

The improvement of GNSS performance in real-time applications, such as navigation, is a widely discussed topic (Bonet et al. 2009; Gaglione et al. 2015); the availability of a large number of contemporary visible satellites allows the reduction of fixing time and improves performances in urban canyons (Angrisano et al. 2009; Gandolfi and La Via 2011).

It is known that precise GNSS positioning can nowadays be performed not only using the differenced approach but also with so-called Precise Point Positioning (PPP) (Geng et al. 2010). The impact of using multi-constellation observables in PPP calculation has been addressed in several publications (Cai et al. 2015; Martín et al. 2011; Rabbou and El-Rabbany 2015; Yu and Gao 2017).

Nevertheless, most technical applications still rely on the classical differencing approach to GNSS observables. Applications using permanent stations rely on long observing sessions, basically for geodesy and augmentation systems for real-time precise positioning, but also for long terms monitoring. Even in these cases, it would be interesting to be aware of the impact of acquiring multiconstellation GNSS observables instead of the usual GPS or GPS/GLONASS-only approach. This topic has been already addressed in Chu and Yang (2014), who consider very long baselines between International GNSS Service (IGS) permanent stations, processed using well-known scientific software for data processing. Moreover, static observing sessions of a few hours can be performed in other applications where permanent stations cannot be installed.

<sup>1</sup>Postdoctoral Research Fellow, Dipartimento di Ingegneria Civile, Chimica, Ambientale e dei Materiali–Univ. of Bologna, Viale Risorgimento 2, 40136 Bologna, Italy (corresponding author). ORCID: <https://orcid.org/0000-0001-8812-5235>. Email: [luca.poluzzi5@unibo.it](mailto:luca.poluzzi5@unibo.it)

<sup>2</sup>Postdoctoral Research Fellow, Dipartimento di Ingegneria Civile, Chimica, Ambientale e dei Materiali–Univ. of Bologna, Viale Risorgimento 2, 40136 Bologna, Italy. Email: [luca.tavasci@unibo.it](mailto:luca.tavasci@unibo.it)

<sup>3</sup>Ph.D. Candidate, Dipartimento di Ingegneria Civile, Chimica, Ambientale e dei Materiali–Univ. of Bologna, Viale Risorgimento 2, 40136 Bologna, Italy. ORCID: <https://orcid.org/0000-0002-6524-9216>. Email: [enrica.vecchi@unibo.it](mailto:enrica.vecchi@unibo.it)

<sup>4</sup>Full Professor, Dipartimento di Ingegneria Civile, Chimica, Ambientale e dei Materiali–Univ. of Bologna, Viale Risorgimento 2, 40136 Bologna, Italy. Email: [stefano.gandolfi@unibo.it](mailto:stefano.gandolfi@unibo.it)

Note. This manuscript was submitted on April 7, 2020; approved on December 14, 2020. **No Epub Date.** Discussion period open until 0, 0; separate discussions must be submitted for individual papers. This paper is part of the *Journal of Surveying Engineering*, © ASCE, ISSN 0733-9453.

65 In this paper, we evaluate the impact of acquiring multiconstel- 91  
66 lation observables in static positioning with a relative approach. 92  
67 These assessments could be useful for dealing with different practical 93  
68 applications. We considered a scenario where 24-h of data files are 94  
69 available and another scenario where only 2-h observing sessions 95  
70 have been performed. The first case can be interesting for those 96  
71 managing a regional GNSS permanent network for deformation 97  
72 monitoring purposes (Cina and Piras 2015), where the distances be- 98  
73 tween the stations typically range between kilometers and tens of 99  
74 kilometers and instruments are mostly installed in positions where 100  
75 sky visibility is good. The tests shown in this paper may help in 101  
76 choosing the instrumentations to install or eventually modernize. 102  
77 A different scenario can be the monitoring of a GNSS network made 103  
78 of passive benchmarks on which the instruments can be set up only 104  
79 for shorter observing sessions of only a few hours. 105

80 The position solutions were obtained using Leica Infinity 106  
81 version 3.2.1 software, which allows baseline computation by se- 107  
82 lecting one or multiple GNSS constellations. Baseline lengths of 108  
83 about 10 and 60 km have been considered. Results are presented 109  
84 and discussed in terms of repeatability of the coordinates (preci- 110  
85 sion) and their consistency in respect to the formal reference posi-  
86 tions (accuracy).

## 87 Dataset

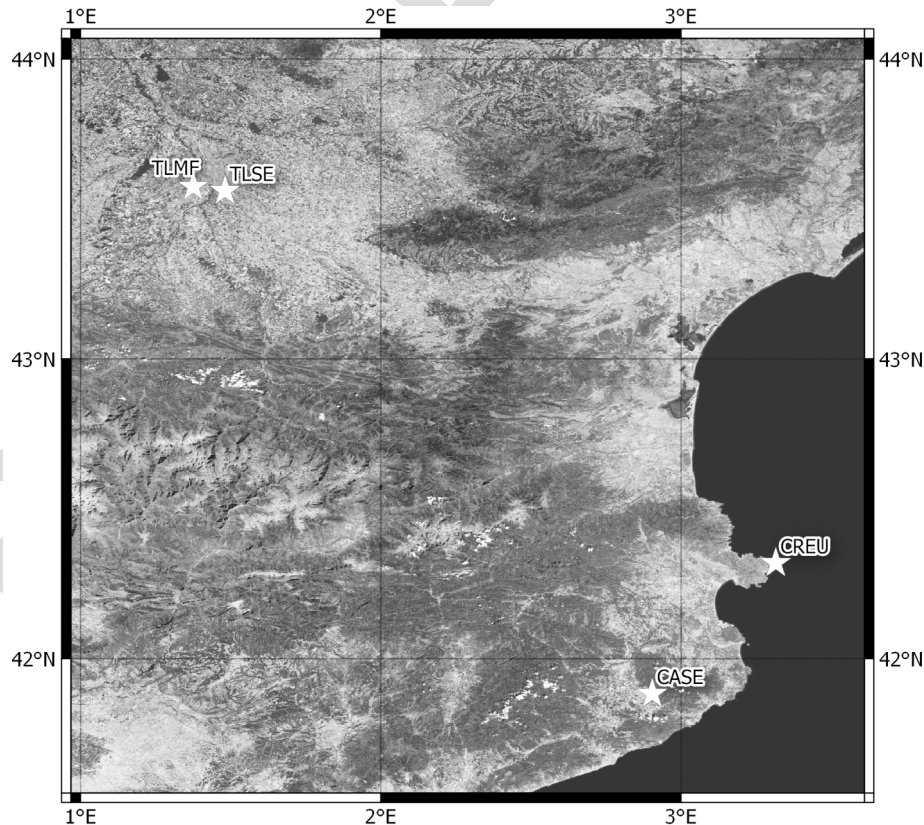
88 GNSS data used for the test were collected by two pairs of perman- 112  
89 ent stations belonging to the European Permanent Network (EPN) 113  
90 (Bruyninx et al. 2019) and located as shown in Fig. 1. The primary 114  
115  
116

91 criterion of this choice has been the availability of multiconstella- 92  
93 tion receivers installed. Moreover, the distances between the se- 94  
95 lected stations are suitable for the test purpose and are 10 and 96  
97 60 km for TLSE-TLMF and CREU-CASE respectively. Ten kilo- 98  
99 meters can be considered a boundary distance for precise surveys 100  
101 with short observing sessions and it is what surveyors may deal 102  
103 with when using GNSS benchmarks to refer their measurements. 104  
105 On the other hand, 60 km is about the maximum distance that one 106  
107 can have from a public permanent station, at least considering 108  
109 national monitoring networks like the Italian Rete Dinamica Nazio- 110  
111 nale (RDN) (Barbarella et al. 2018). Longer baselines have not  
112 been considered because typically these are computed for geodetic  
113 purposes using scientific software packages.

104 Daily Receiver Independent Exchange Format (*RINEX*) files 105  
106 with 30-s rate observations were downloaded for a period ranging 107  
108 from the beginning of March 2018 to the end of February 2019. 109  
110 Starting from these files, a 2-h *RINEX* per day was created for each 111  
112 day, which simulates an independent observing session shorter than 113  
114 24-h. Table 1 shows the main information about the hardware and 115  
116 the type of provided data for the considered permanent stations.

## GNSS Data Processing

112 The GNSS data processing was performed by Infinity software, 113  
114 which has been recently introduced on the market by Leica Geo- 115  
116 systems. Infinity is a geospatial office suite designed to manage, 117  
118 process, and analyze GNSS data and other observations acquired 119  
120 by topographic instruments such as Total Stations, Digital Levels,



Map created with QGIS, map data by ESRI World Imagery © Esri, DigitalGlobe, GeoEye, Earthstar Geographics, CNES/Airbus DS, USDA, USGS, AeroGRID, IGN, and the GIS User Community.

F1:1 **Fig. 1.** Location of GNSS permanent stations considered for the test. (Map created with QGIS, map data by ESRI World Imagery © Esri, 117  
F1:2 DigitalGlobe, GeoEye, Earthstar Geographics, CNES/Airbus DS, USDA, USGS, AeroGRID, IGN, and the GIS User Community.) 118

**Table 1.** GNSS permanent stations considered for the test: features and equipment

| T1:1 | Station         | TLSE                         | TLMF             | CREU                         | CASE                         |
|------|-----------------|------------------------------|------------------|------------------------------|------------------------------|
| T1:2 | Baseline length | 10 km                        |                  | 60 km                        |                              |
| T1:3 | Receiver        | TRIMBLE NETR9                | LEICA GR25       | LEICA GR50                   | LEICA GR50                   |
| T1:4 | Antenna radome  | TRM59800.00 NONE             | TRM57971.00 NONE | LEIAR25.R4 NONE              | LEIAR25.R4 NONE              |
| T1:5 | Data type       | Daily, hourly, and real-time | Daily and hourly | Daily, hourly, and real-time | Daily, hourly, and real-time |

**Table 2.** Combinations of GNSS observables and frequencies that Leica Infinity used for each type of solution

| T2:1 | ID            | Constellations             | Used frequencies                     |
|------|---------------|----------------------------|--------------------------------------|
| T2:2 | G             | GPS                        | L1/L2/L5                             |
| T2:3 | R             | GLONASS                    | L1/L2                                |
| T2:4 | E             | GALILEO                    | E1/E5a/E5b/E5a+b                     |
| T2:5 | C             | BEIDOU                     | B1/B2                                |
| T2:6 | G + R         | GPS+GLONASS                | Combination of the above frequencies |
| T2:7 | G + E         | GPS+GALILEO                |                                      |
| T2:8 | G + R + E     | GPS+GLONASS+GALILEO        |                                      |
| T2:9 | G + R + E + C | GPS+GLONASS+GALILEO+BEIDOU |                                      |

117 and Unmanned Aerial Vehicles (UAVs). As for the GNSS data  
 118 processing, the software allows the processing of the main global  
 119 constellations, in particular: GPS, GLONASS, Galileo, and BeiDou.  
 120 Data from different constellations can be combined or independently  
 121 processed per the user's choice.

122 The Multi-GNSS Experiment (MGEX) ephemeris were down-  
 123 loaded (sp3 file format) to allow the processing of all the observ-  
 124 ables (NASA 2021). Absolute antenna calibrations provided by  
 125 National Geodetic Survey (NGS) were used and a 13° cut-off angle  
 126 was chosen. As for the troposphere modeling, the Vienna Mapping  
 127 Function (Kouba 2008) was implemented using Global Pressure  
 128 and Temperature model (GPT2) files and the Calculated option  
 129 was selected for the signals delay estimation according to the  
 130 software user manual in the case of long baselines ( $\geq 10$  km). The  
 131 impact of the ionosphere is considered in Infinity by using an iono-  
 132 free frequency combination. The option that enables the application  
 133 of NGS 14 antenna calibrations was also selected.

134 Eight types of baseline solutions were calculated to evaluate the  
 135 impact of a single constellation or a particular combination of these.  
 136 Table 2 presents the constellations used for each type of solution.

137 The Earth-Centered Earth-Fixed (ECEF) coordinates ( $X, Y, Z$ )  
 138 expressed in the European Terrestrial Reference Frame (ETRF2000)  
 139 at the epoch 2010.0, and the related velocities ( $V_x, V_y, V_z$ ) for  
 140 each GNSS station are published in the European Reference Frame  
 141 website (EUREF 2021). These positions, expressed at each meas-  
 142 urement epoch within the considered period, were used as reference  
 143 positions for the master stations.

## 144 Data Analysis and Results

145 After data processing, the rover solutions were stacked into coord-  
 146 inate time series and analyzed to evaluate the precision in terms  
 147 of the estimated coordinates repeatability. The time series were  
 148 cleaned from the outlier solutions by following an automated re-  
 149 jection criterion based on the assumption of linear variation of  
 150 the coordinates over time and Gaussian distribution of the residuals.

151 We denoted  $S_i^j(t)$  to be the value of the geodetic component  $i$  ( $I =$   
 152 North, East, Up) related to the rover station  $j$  ( $j =$  TLMF, CASE) at  
 153 epoch  $t$ . We set  $S_i^j = \{S_i^j(t_1), S_i^j(t_2), \dots, S_i^j(t_n)\}, t_i < t_j$  for  $i < j$   
 154 to form a time series for each coordinate. The position models  
 155  $mod_i^j$  were derived using Eq. (1), where  $m_i^j$  and  $q_i^j$  represent the

slope and the intercept of the regression straight line of each time  
 156 series, respectively. These parameters were estimated using a  
 157 classical Least Squares approach  
 158

$$mod_i^j(t) = q_i^j + t m_i^j \quad (1)$$

**Table 3.** Averaged discards between rover solutions and formal ETRF2000 reference solutions

| Time span (h) | Rover solution | Constellations | Accuracy (mm) |      |       |       |       |
|---------------|----------------|----------------|---------------|------|-------|-------|-------|
|               |                |                | N             | E    | U     |       |       |
| 2             | TLMF           | C              | 3.0           | 8.0  | 25.2  | T3:1  |       |
|               |                | E              | 4.4           | 3.5  | 33.4  | T3:2  |       |
|               |                | R              | 3.0           | 0.5  | 28.8  | T3:3  |       |
|               |                | G              | 4.0           | 0.8  | 27.1  | T3:4  |       |
|               |                | G + E          | 3.6           | 0.9  | 26.9  | T3:5  |       |
|               |                | G + R          | 3.5           | 0.7  | 26.5  | T3:6  |       |
|               |                | G + R + E      | 3.5           | 0.8  | 26.8  | T3:7  |       |
|               |                | G + R + E + C  | 3.4           | 0.9  | 26.6  | T3:8  |       |
|               |                | CASE           | C             | 13.3 | 16.8  | 35.4  | T3:9  |
|               | E              | 7.0            | 0.0           | 13.8 | T3:10 |       |       |
|               | R              | 9.5            | 0.9           | 14.9 | T3:11 |       |       |
|               | G              | 6.7            | 1.1           | 7.8  | T3:12 |       |       |
|               | G + E          | 4.8            | 0.0           | 7.8  | T3:13 |       |       |
|               | G + R          | 4.5            | 0.1           | 7.8  | T3:14 |       |       |
|               | G + R + E      | 4.8            | 0.0           | 6.8  | T3:15 |       |       |
|               | G + R + E + C  | 4.7            | 0.0           | 6.4  | T3:16 |       |       |
|               | 24             | TLMF           | C             | 3.5  | 0.3   | 24.8  | T3:17 |
|               |                |                | E             | 4.4  | 3.4   | 31.8  | T3:18 |
| R             |                |                | 2.8           | 0.1  | 27.4  | T3:19 |       |
| G             |                |                | 3.3           | 0.4  | 26.9  | T3:20 |       |
| G + E         |                |                | 3.2           | 0.5  | 28.0  | T3:21 |       |
| G + R         |                |                | 3.1           | 0.3  | 26.8  | T3:22 |       |
| G + R + E     |                |                | 3.2           | 0.4  | 26.0  | T3:23 |       |
| G + R + E + C |                |                | 3.3           | 0.3  | 27.1  | T3:24 |       |
| CASE          |                |                | C             | 9.1  | 3.4   | 6.3   | T3:25 |
| E             |                | 6.2            | 0.2           | 13.9 | T3:26 |       |       |
| R             |                | 7.4            | 1.5           | 14.3 | T3:27 |       |       |
| G             |                | 5.5            | 0.0           | 7.8  | T3:28 |       |       |
| G + E         |                | 5.7            | 0.1           | 8.8  | T3:29 |       |       |
| G + R         |                | 6.0            | 0.2           | 8.3  | T3:30 |       |       |
| G + R + E     |                | 6.0            | 0.1           | 8.4  | T3:31 |       |       |
| G + R + E + C |                | 6.1            | 0.1           | 7.4  | T3:32 |       |       |

159 We defined the residual  $v_i^j(t)$  as the difference between each  
 160 coordinate and the model at the same epoch

$$v_i^j(t) = S_i^j(t) - \text{mod}_i^j(t) \quad (2)$$

161 Then,  $\sigma_i^j$  was assumed to be the RMS of the residuals  $v_i^j$  for each  
 162 component and station. We adopted an iterative procedure based on  
 163 the comparison between the maximum residual and the RMS of the  
 164 related time series to identify possible outliers. Therefore, a residual  
 165 is an outlier if

$$\max\{v_i^j | \text{abs}(v_i^j) > 3\sigma_i^j\} \quad (3)$$

166 All the three components of a solution were removed if just one  
 167 of these represented an outlier. The models, the associated residuals  
 168 and the  $\sigma_i^j$  values were recalculated iteratively after each outlier  
 169 rejection and the precision parameter of the data series can be rep-  
 170 resented by the final value of  $\sigma_i^j$ .

171 In order to evaluate the accuracy of the baseline solutions, the  
 172 discards between the rover coordinates  $S_i^j(t)$  and the related  
 173 ETRF2000 reference values were also computed. The average of  
 174 these discards represent the accuracy of the calculated baselines  
 175 and are reported in Table 3.

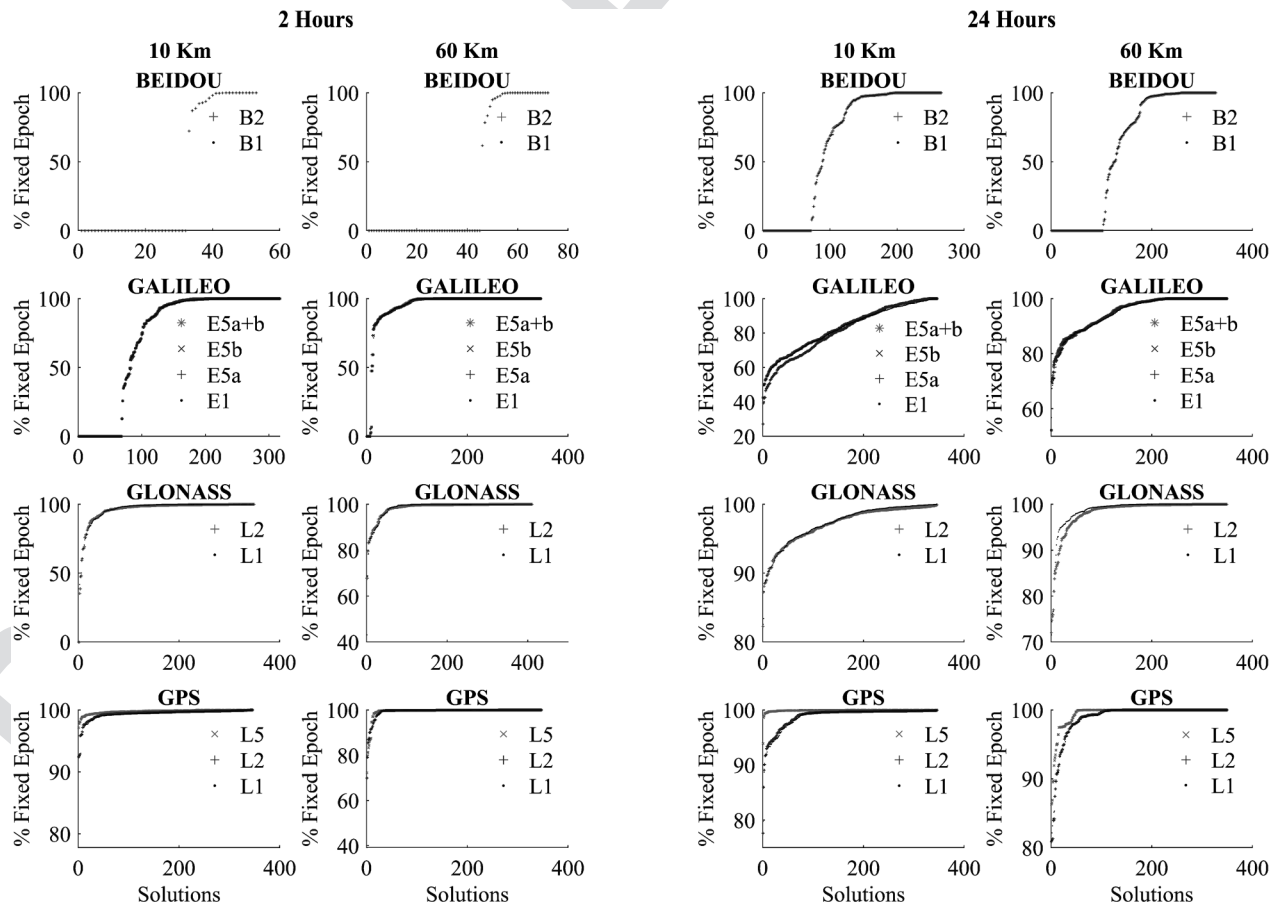
176 By looking at the plan components (i.e. North and East), the  
 177 estimated baselines seem to be highly accurate in the East direction,  
 178 with a few mm biases toward the South, that are larger for the  
 179 60-km-long baselines. As for the Up direction, the CREU-CASE  
 180 baselines are coherent with respect to the references within one cm.  
 181 On the contrary, the TLSE-TLMF baselines show unexpected biases

with a magnitude of more than 2 cm. This may be due to some soft-  
 ware bugs in the application of metadata concerning the antenna  
 offsets or the antenna calibrations. The only constellation that pro-  
 duces significantly biased solutions in all the components is the  
 Beidou one, especially considering the longer baseline and the 2-h  
 time span. This can be explained by looking at Fig. 2, which shows  
 the percentage of epochs with fixed ambiguities for each baseline  
 solution depending on the GNSS constellation. All solutions were  
 reordered starting from the lower percentages of epochs with fixed  
 ambiguities instead of chronologically to allow an easier evaluation  
 of the results. The Fig. 2 points out how the processing of Beidou  
 data is characterized by a high percentage of solutions estimated  
 with float ambiguities.

The main results are summarized in Table 4, concerning both  
 the length of the baseline and both the observing session time spans  
 considered for the test. These results confirm the well-known  
 dependency of the precision on the baseline length (Eckl et al. 2001;  
 Anjasmara et al. 2019), where the longest baseline has a scattering  
 about the double concerning the shorter one.

The GPS still provides the most precise results among the single  
 constellations, especially looking at the height component. Never-  
 theless, the GLONASS system gives very similar precisions in the  
 horizontal components, and also the Galileo constellation shows  
 repeatability of the position solutions close to the previous ones.

Despite the good values of the dilution of precision (DOP)  
 parameters, a high percentage of Galileo solutions calculated from  
 the 2-h files were rejected. Moreover, these solutions are highly  
 scattered along the Up direction, showing  $\sigma_{Up}^j$  values that are



F2:1 **Fig. 2.** Charts of the percentage of fixed epochs for each solution for 2- and 24-h time spans. Values on the x-axis are sorted in order to have increasing  
 F2:2 percentage of fixed epochs.

**Table 4.** Overall statistics for each type of baseline and time span: precisions (columns 4–6), DOP values (columns 7 and 8), mean number of satellites (column 9), total number of processed solution (column 10), and percentage of rejected solutions (column 11)

|       | Time span (h) | Baseline (km) | Constellations | $\sigma_N$ (mm) | $\sigma_E$ (mm) | $\sigma_U$ (mm) | HDOP | VDOP | MNS  | $n^\circ$ sol | % rej |
|-------|---------------|---------------|----------------|-----------------|-----------------|-----------------|------|------|------|---------------|-------|
| T4:1  |               |               |                |                 |                 |                 |      |      |      |               |       |
| T4:2  | 24            | 10            | C              | 4.8             | 5.9             | 18.3            | 6.2  | 8.3  | 3.6  | 266           | 39.8  |
| T4:3  |               |               | E              | 1.3             | 2.4             | 6.4             | 2.1  | 2.7  | 5.8  | 346           | 4     |
| T4:4  |               |               | R              | 0.9             | 1.8             | 4.2             | 1.0  | 1.5  | 8.4  | 346           | 3.2   |
| T4:5  |               |               | G              | 0.9             | 1.9             | 2.9             | 0.9  | 1.2  | 11.0 | 346           | 2.0   |
| T4:6  |               |               | G + E          | 0.8             | 1.8             | 2.5             | 0.7  | 0.9  | 16.8 | 346           | 3.5   |
| T4:7  |               |               | G + R          | 0.8             | 1.8             | 2.4             | 0.6  | 0.8  | 19.3 | 346           | 2.6   |
| T4:8  |               |               | G+R+E          | 0.8             | 1.8             | 2.5             | 0.5  | 0.7  | 25.1 | 346           | 2.0   |
| T4:9  |               |               | G+R+E+C        | 0.8             | 1.9             | 2.6             | 0.4  | 0.6  | 28.7 | 346           | 2.0   |
| T4:10 |               | 60            | C              | 27.5            | 35.6            | 51.1            | 6.2  | 8.3  | 3.8  | 327           | 33.5  |
| T4:11 |               |               | E              | 2.8             | 2.0             | 7.8             | 1.9  | 2.5  | 7.2  | 349           | 10    |
| T4:12 |               |               | R              | 2.2             | 2.0             | 6.6             | 1.0  | 1.5  | 8.6  | 349           | 10.9  |
| T4:13 |               |               | G              | 2.5             | 1.8             | 5.1             | 0.9  | 1.2  | 11.0 | 349           | 4.9   |
| T4:14 |               |               | G+E            | 2.5             | 1.9             | 4.6             | 0.7  | 0.9  | 18.2 | 349           | 5.7   |
| T4:15 |               |               | G+R            | 2.4             | 1.9             | 4.5             | 0.6  | 0.8  | 19.6 | 349           | 5.2   |
| T4:16 |               |               | G+R+E          | 2.4             | 2.0             | 4.5             | 0.5  | 0.7  | 26.8 | 349           | 8.6   |
| T4:17 |               |               | G+R+E+C        | 2.5             | 2.1             | 5.0             | 0.4  | 0.6  | 30.6 | 349           | 7.2   |
| T4:18 | 2             | 10            | C              | 26.6            | 40.0            | 38.0            | 4.1  | 5.4  | 3.0  | 53            | 38.9  |
| T4:19 |               |               | E              | 2.8             | 3.8             | 19.7            | 1.8  | 2.6  | 5.0  | 318           | 26.1  |
| T4:20 |               |               | R              | 1.7             | 2.4             | 10.9            | 0.9  | 1.4  | 7.1  | 349           | 7.7   |
| T4:21 |               |               | G              | 1.9             | 2.4             | 6.5             | 0.8  | 1.2  | 9.2  | 346           | 5.8   |
| T4:22 |               |               | G+E            | 1.9             | 2.4             | 5.8             | 0.7  | 0.9  | 14.2 | 346           | 4.3   |
| T4:23 |               |               | G+R            | 1.6             | 2.3             | 5.2             | 0.6  | 0.8  | 16.3 | 349           | 7.2   |
| T4:24 |               |               | G+R+E          | 1.5             | 2.2             | 4.9             | 0.5  | 0.7  | 21.3 | 349           | 5.2   |
| T4:25 |               |               | G+R+E+C        | 1.5             | 2.3             | 4.8             | 0.5  | 0.7  | 24.3 | 349           | 5.7   |
| T4:26 |               | 60            | C              | 66.2            | 118.5           | 124.4           | 2.5  | 4.6  | 2.9  | 72            | 23.7  |
| T4:27 |               |               | E              | 5.4             | 3.9             | 27.8            | 1.4  | 2.0  | 6.1  | 338           | 17.5  |
| T4:28 |               |               | R              | 4.6             | 3.7             | 22.3            | 1.0  | 1.5  | 7.1  | 347           | 4.3   |
| T4:29 |               |               | G              | 4.3             | 3.2             | 12.4            | 0.9  | 1.2  | 9.7  | 347           | 9.0   |
| T4:30 |               |               | G+E            | 4.2             | 3.3             | 11.4            | 0.6  | 0.9  | 15.8 | 347           | 8.4   |
| T4:31 |               |               | G+R            | 4.2             | 3.2             | 10.5            | 0.6  | 0.8  | 16.8 | 347           | 8.9   |
| T4:32 |               |               | G+R+E          | 4.2             | 3.2             | 10.4            | 0.5  | 0.7  | 22.9 | 347           | 8.1   |
| T4:33 |               |               | G+R+E+C        | 4.1             | 3.2             | 10.1            | 0.4  | 0.6  | 25.7 | 347           | 9.2   |

up to triple the GPS ones. Note that in most cases the BeiDou constellation shows a dispersion of the solutions one order of magnitude higher than the other GNSS constellations, also presenting the highest percentages of outliers. These results are certainly not due to a malfunction of the Chinese positioning system but they depend on the low number of acquired satellites and their geometry considering the chosen cut-off angle. The weakness of the BeiDou satellite geometry is also evidenced by the DOP parameters and probably is the cause of the low percentage of fixed solutions shown in Fig. 2 and the consequent poor accuracy of the solutions. Nevertheless, it could also be due to some problem with the MGEX ephemeris, which are not verifiable using our dataset.

Fig. 3 emphasizes the results in terms of precision of the baselines and their correlation with the quality of the satellite geometry, represented through the DOP parameters. As for the results obtained from 24-h data files, the use of all constellations does not produce significant improvement of the precision. The GPS-GLONASS combination is the one giving the best results, but the difference concerning the other combinations seems to be negligible. The only improvement due to the use of the multiconstellation is on the height component, which is slightly more precise than the single GPS.

A comparison of the results obtained shows that the use of GPS with Galileo improves the precision on the height component and reduces the percentages of outlier solutions with respect to only the Galileo constellation. Very similar considerations can also be done for the GLONASS with respect to the GPS-GLONASS combination.

As for the test concerning 2-h *RINEX* files, the baseline solutions are significantly less precise with respect to those estimated with 24-h observations. The reduced amount of data strongly impacts mainly on the BeiDou results for the 60-km baseline. It is worth noting that in the case of 2-h processing, even the BeiDou constellation slightly improves the precision of the full constellation combined solution, despite its own performances being scattered. Galileo performances are a bit worsened by the reduced observing session, especially considering the height component with respect to GPS ones. Nevertheless, Galileo allows precisions of the same order of magnitude of what GPS and GLONASS do, and can help improve the performances in the case of combining multiconstellation observables. This is not the case when considering 24-h observations, where the most precise solution is achieved by using GPS and GLONASS constellations only.

## Discussion and Conclusion

The impact of using different GNSS constellations and their different combinations has been investigated in this paper by computing two baselines of different lengths over a period of one year using daily and 2-h *RINEX* files. A possible application of the test results is to help surveyors dealing with regional GNSS networks evaluating the advantages of using new full-constellation instrumentations instead of older ones. Two pairs of CORS stations of the EUREF network define these baselines (TLSE-TLMF, CREU-CASE). Each station acquires data from four constellations (GPS,

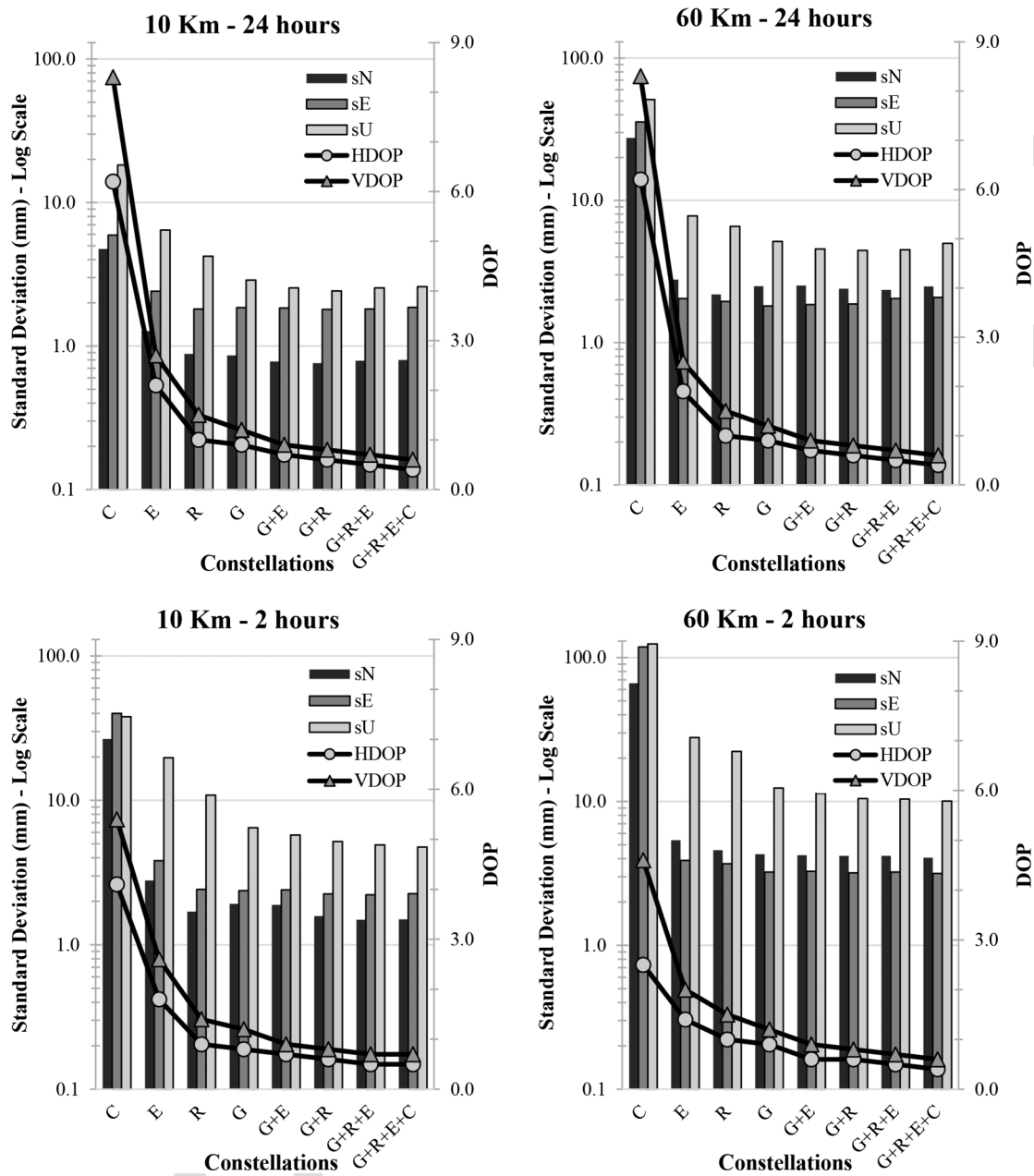


Fig. 3. Charts and histograms of the precision and DOP parameters for each analyzed solution.

F3:1

263 Glonass, Galileo, and Beidou) with a 30-s sampling rate. Data  
 264 processing was performed using the Leica Infinity commercial  
 265 software.

266 The test results show that the use of multiple constellations does  
 267 not have a strong impact on the precision of solutions based on 24-h  
 268 of observations, at least for the considered baseline lengths that are  
 269 10 and 60 km. Indeed the main advantage of using multiconstel-  
 270 lation is to increase the number of observables acquired by the  
 271 receivers, which is not a critical aspect for very long observing ses-  
 272 sions but has been observed to impact positively on 2-h acquisitions.  
 273 In this case, adding the observables of constellations such  
 274 as Beidou to the combined processing, which does not provide suit-  
 275 able results by itself, helps to improve the precisions.

276 Considering single-constellation solutions, the GPS one is still  
 277 providing the best precision, especially on the height component.  
 278 Nevertheless, both the GLONASS and the Galileo constellations  
 279 provide just slightly less precise results, so they can certainly be

280 considered alternatively to GPS for the presented application.  
 281 The European constellation shows a weakness in the height compo-  
 282 nent with respect to the GPS, which is enhanced in the case of  
 283 processing 2-h observations. The BeiDou constellation shows sig-  
 284 nificantly worse precisions with respect to the others, but its per-  
 285 formances actually cannot be criticized given that they were  
 286 affected by a poor number of satellites and a weak geometry over  
 287 the considered area.

288 Bearing in mind that multiple constellations would probably  
 289 have higher impact in more demanding situations with respect  
 290 to the test scenarios, such as very long baselines or poor sky vis-  
 291 ibility, we can conclude that the use of multiconstellation GNSS  
 292 instead of GPS-only provides a slight advantage in terms of pre-  
 293 cision in the case of 24-h data processing, typical of permanent  
 294 stations. In this case, adding the Galileo observables in the com-  
 295 putation of daily static solutions does not provide any advantage  
 296 in terms of precision at the time, at least when using Leica Infinity

297 software. Additionally, for the applications involving shorter  
298 observing sessions, the combined use of Galileo observables to-  
299 gether with others improves the baseline precision. Moreover, the  
300 availability of the Galileo constellation may be a major advantage  
301 thanks to the civilian vocation of the European GNSS because it  
302 can provide integrity services that may be fundamental for survey  
303 certification.

### 304 Data Availability Statement

305 All GNSS data (*RINEX* and *ephemeris* files) used during the study  
306 are available in a repository or online in accordance with funder  
307 data retention policies (*RINEX*: <ftp://ftp.epncb.oma.be/pub/obs/>;  
308 *ephemeris*: <ftp://cddis.gsfc.nasa.gov/pub/gps/products/mgex/>). The  
309 GNSS processing code used during the study was provided by a  
310 third party (Infinity–Leica Geosystems); direct request for these  
311 materials may be made to the provider as indicated in the Acknowl-  
312 edgments. All the data analysis codes that support the findings of  
313 this study are available from the corresponding author upon reason-  
314 able request.

### 315 Acknowledgments

316 We would like to show our gratitude to Leica Geosystem Italia for  
317 making Infinity software available for GNSS data processing.

### 318 References

319 Angrisano, A., S. Gaglione, A. Pacifico, and M. Vultaggio. 2009. "Multi-  
320 constellation system as augmentation to GPS performance in difficult  
321 environment or critical application." In *Proc., ENC-GNSS-09*, 1–10.  
322 Rome: Istituto italiano di navigazione.

323 Anjasmara, I. M., D. G. Pratomo, and W. Ristanto. 2019. "Accuracy analy-  
324 sis of GNSS (GPS, GLONASS and BEIDOU) observation for position-  
325 ing." In Vol. 94 of *Proc., E3S Web Conf.*, 1019. Les Ulis, France: EDP  
326 Sciences.

327 Barbarella, M., S. Gandolfi, and L. Tavasci. 2018. *Monitoring of the Italian*  
328 *GNSS geodetic reference frame*. Cham, Switzerland: Springer.

329 Bonet, B., I. Alcantarilla, D. Flament, C. Rodriguez, and N. Zarraoa. 2009.  
330 "The benefits of multi-constellation GNSS: Reaching up even to single  
331 constellation GNSS users." In *Proc., 22nd Int. Technical Meeting of the*  
332 *Satellite Division of the Institute of Navigation 2009, ION GNSS 2009*,  
333 936–948. Savannah, GA: Institute of Navigation.

Bruyninx, C., J. Legrand, A. Fabian, and E. Pottiaux. 2019. "GNSS meta-  
data and data validation in the EUREF permanent network." *GPS*  
*Solutions* 23 (4): 1–14. <https://doi.org/10.1007/s10291-019-0880-9>.

Cai, C., Y. Gao, L. Pan, and J. Zhu. 2015. "Precise point positioning with  
quad-constellations: GPS, BeiDou, GLONASS and Galileo." *Adv.*  
*Space Res.* 56 (1): 133–143. <https://doi.org/10.1016/j.asr.2015.04.001>.

Chu, F. Y., and M. Yang. 2014. "GPS/Galileo long baseline computation:  
Method and performance analyses." *GPS Solutions* 18 (2): 263–272.  
<https://doi.org/10.1007/s10291-013-0327-7>.

Cina, A., and M. Piras. 2015. "Performance of low-cost GNSS receiver for  
landslides monitoring: Test and results." *Geomatics Nat. Hazards Risk*  
6 (5–7): 497–514. <https://doi.org/10.1080/19475705.2014.889046>.

Eckl, M. C., R. A. Snay, T. Soler, M. W. Cline, and G. L. Mader. 2001.  
"Accuracy of GPS-derived relative positions as a function of interstation  
distance and observing-session duration." *J. Geod.* 75 (12): 633–640.  
<https://doi.org/10.1007/s001900100204>.

EUREF (Regional Reference Frame Sub-Commission for Europe). 2021.  
"EUREF permanent GNSS network—Station list." Accessed February  
9, 2021. [http://www.epncb.oma.be/\\_networkdata/stationlist.php](http://www.epncb.oma.be/_networkdata/stationlist.php).

Gaglione, S., A. Angrisano, P. Freda, A. Innac, M. Vultaggio, and N.  
Crocetto. 2015. "Benefit of GNSS multiconstellation in position and  
velocity domain." In *Proc., 2nd IEEE Int. Workshop on Metrology*  
*for Aerospace, MetroAeroSpace 2015*, 9–14. New York: IEEE.

Gandolfi, S., and L. La Via. 2011. "SKYPLOT-DEM: A tool for GNSS  
planning and simulations." *Appl. Geomatics* 3 (1): 35–48. <https://doi.org/10.1007/s12518-011-0045-1>.

Geng, J., X. Meng, F. Teferle, and A. Dodson. 2010. "Performance of pre-  
cise point positioning with ambiguity resolution for 1-to 4-hour obser-  
vation periods." *Surv. Rev.* 42 (316): 155–165. <https://doi.org/10.1179/003962610X12572516251682>.

Kouba, J. 2008. "Implementation and testing of the gridded Vienna map-  
ping function 1 (VMF1)." *J. Geod.* 82 (4–5): 193–205. <https://doi.org/10.1007/s00190-007-0170-0>.

Martín, A., A. B. Anquela, R. Capilla, and J. L. Berné. 2011. "PPP tech-  
nique analysis based on time convergence, repeatability, IGS products,  
different software processing, and GPS+GLONASS constellation." *J. Surv. Eng.* 137 (3): 99–108. [https://doi.org/10.1061/\(ASCE\)SU.1943-5428.0000047](https://doi.org/10.1061/(ASCE)SU.1943-5428.0000047).

NASA (National Aeronautics and Space Administration). 2021. Archive of  
space geodesy data—CDDIS (the crustal dynamics data information  
system)." Accessed February 9, 2021. [http://www.epncb.oma.be/\\_networkdata/stationlist.php](http://www.epncb.oma.be/_networkdata/stationlist.php).

Rabbou, M. A., and A. El-Rabbany. 2015. "Precise point positioning using  
multi-constellation GNSS observations for kinematic applications." *J. Appl. Geod.* 9 (1): 15–25. <https://doi.org/10.1515/jag-2014-0021>.

Yu, X., and J. Gao. 2017. "Kinematic precise point positioning using multi-  
constellation global navigation satellite system (GNSS) observations." *Int. J. Geo-Informat.* 6 (1): 6.